Journal of Solid State Electrochemistry
https://doi.org/10.1007/s10008-017-3861-3

ORIGINAL PAPER

On the electrochemical activity of β-lead dioxide in sulfuric acid solution: a comparative study between the chemical and electrochemical routes

I. Derafa[1] · L. Zerroual[1] · M. Matrakova[2]

Received: 21 September 2017 / Revised: 5 December 2017 / Accepted: 9 December 2017

Abstract
β-Lead dioxide is prepared by chemical and electrochemical routes. The chemical sample is obtained by dissolving lead tetra-acetate in distilled water at room temperature. The electrochemical sample is prepared by oxidizing cured plates in sulfuric acid with 1.05 g cm^{-3} specific gravity. The two powders are indexed as β-PbO_2. The sample prepared by chemical route presents smaller crystallite size. When cycling the two powders up to 100 cycles between 0.5 and 1.5 V versus Hg/Hg_2SO_4 reference electrode, the electrochemical sample presents higher values of anodic and cathodic peak current densities and higher discharge capacity. Thermal analysis and electrochemical techniques are used to explain this difference in activity between the two samples.

Keywords Lead dioxide · X-ray diffraction · Capacity · Crystallite size · Structural water

Introduction

Anodically formed dioxide coatings on lead and its alloys comprise a mixture of two polymorphic forms of PbO_2: orthorhombic α-PbO_2 and tetragonal β-PbO_2 [1, 2]. In the conventional process, the formation of PbO_2 starts at the interface grid/electrolyte in the corrosion layer then advances in the cured paste. The relative amounts of the two polymorphs of PbO_2 depend on the conditions of manufacture, i.e., positive paste density, specific gravity, and temperature of the formation acid, as well as formation rate.

The stability of α- and β-PbO_2 in sulfuric acid was determined by Rüetschi et al. [3]; orthorhombic α-PbO_2 was found to be considerably less stable than tetragonal β-PbO_2. Both modifications readily reduce electrochemically to $PbSO_4$, and the discharge capacity of α-form is lower than that of β-PbO_2.

✉ L. Zerroual
zerroual@yahoo.fr

[1] Laboratoire d'Energétique et Electrochimie du Solide (LEES), Faculté´ de Technologie, Université´ Ferhat ABBAS, 19000 Sétif, Algeria

[2] Institute of electrochemistry and energy systems (IEES), Bulgarian Academy of Sciences, 1113 Sofia, Bulgaria

Many studies have been reported in the literature concerning the electrochemical activity of both chemical and electrochemical positive active material. Compared with chemically prepared PbO_2, which is reputed to be electrochemically less active form, material prepared by electrochemical formation of positive plates of lead/acid batteries exhibits high electrochemical activity. It was found that in general electrochemically prepared lead dioxide is non-stoichiometric, whereas chemically prepared PbO_2 is nearly stoichiometric [4, 5].

The origin of the electrochemical activity of lead dioxide was largely documented in the literature. Caulder et al. [6] studied the effect of thermal decomposition of formed and cycled lead dioxide electrodes on the capacity loss and battery failure. They made in evidence the existence of an electrochemically active amorphous form of PbO_2. When cycled to failure, it is converted to an electrochemically inactive form of PbO_2. This later form of PbO_2 gives DTA results similar to those obtained on chemical reagent PbO_2. Turner et al. [7] confirmed that chemically prepared PbO_2 can be used to give capacity with a utilization similar to that of commercial electrochemically formed plates. Taylor et al. [8, 9] proposed a process for making positive battery plates not requiring curing or formation and using high surface area chemically prepared lead dioxide mixed with TTB or lead sulfate. Successful use of chemically prepared PbO_2 is demonstrated.

Published online: 19 December 2017

Moseley and Bridger [10] showed that chemically prepared PbO_2 can be used for both flat and tubular plates. In the case of flat plates, the function of the curing process will need to be replaced by a binder to hold the active material in place, but for tubular cells, it should be possible to pour neat powder in the separator bags, which will retain the active mass in position.

Other researchers comparing chemically and electrochemically prepared PbO_2 found amorphous parts of lead dioxide in the electrochemically prepared sample [11]. The decrease of positive plate capacity was related to the conversion of the active amorphous lead dioxide to the inactive crystalline form during cycling. Tokunaga et al. [12] found that when anisotropic graphite is added to the positive paste, the porosity of the positive active mass increased. In addition, its capacity increases remarkably and also cycle life was improved.

Rüetschi [13] studied the effect of crystal structure and interparticle contact on the capacity of chemically prepared samples of α-PbO_2 and β-PbO_2 mixed with various quantities of graphite. He concluded that electrodes of α-PbO_2 with high degree of structural disorder presented a higher discharge performance than those of well-crystallized β-PbO_2. A new concept which views the structure of PAM as a gel-crystal system with electron and proton conductivity has been proposed by Pavlov [14]. The same author in collaboration with his coworkers [15] found that gel zones represent more than 30% of the surface layer of PbO_2.

Monahov et al. [16] made in evidence the existence of hydrated structures in the anodic layer formed on lead electrodes in H_2SO_4 solution. At a given potential, Pb^{4+} ions are formed on the electrode surface. These are unstable in aqueous solutions and form $Pb(OH)_4$. The $Pb(OH)_4$ is dehydrated partially or completely giving $PbO(OH)_2$ and PbO_2. The electrode surface is covered by a layer of PbO_2, $PbO(OH)_2$, and $Pb(OH)_4$, which layer has gel-like properties.

Pavlov [14] proposed that during the discharge of the positive battery plate, the reduction of $PbO(OH)_2$ to $PbSO_4$ proceeds in two stages. The first is electrochemical and occurs in the bulk of the agglomerates and particles and gives $Pb(OH)_2$ according to Eq. (1):

$$PbO(OH)_2 + 2H^+ + 2\,e^- \rightarrow Pb(OH)_2 + H_2O \quad (1)$$

During the second stage, $PbSO_4$ formation takes place through a chemical reaction between $Pb(OH)_2$ and H_2SO_4. It can be expressed by Eq. (2):

$$Pb(OH)_2 + H_2SO_4 \rightarrow PbSO_4 + 2H_2O \quad (2)$$

In a previous work [17] using an all solid-state system exempt of H_2SO_4 and combining the kinetic tests and coulometric measurements, we showed that the mechanism of PAM reduction includes two electrochemical stages (one electron is consumed during each stage) taking place in the gel zones according to a proton-electron mechanism or a double-injection process as indicated in Eqs. (3) and (4):

$$PbO_2 + H^+ + e^- \rightarrow PbOOH \quad (3)$$

$$PbOOH + H^+ + e^- \rightarrow Pb(OH)_2 \quad (4)$$

In the light of these findings, it follows that such a mechanism may be possible only if PbO_2 is both electron and proton conductive. The role of structural water in the activity of the positive active material has been emphasized by many authors. Hill et al. [18] examined PbO_2 samples taken from positive plates of lead-acid batteries and reported that hydrogen is incorporated by surface hydrolysis during crystal growth. In their studies on the role of hydration water in the reduction process of α- and β-lead dioxide on the capacity loss, Fitas et al. [19–21] showed that the removal of the OH^- groups from β-PbO_2 needs an energy twice that of the α-form. In addition, the capacity decreased when structural water is removed. This loss of capacity is important when α-PbO_2 samples are considered.

In our previous work [22], we used an all solid-state system and estimated the proton diffusion coefficient for both fresh and heat-treated α- and β-PbO_2 samples. We demonstrated that the removing of structurally bonded water affects considerably the electrochemical properties of PbO_2 and leads to a decrease in the value of the proton diffusion coefficient. A new mechanism of PbO_2 reduction was proposed.

In their work, Morales et al. [23] prepared lead dioxide samples with particles ranging from nanometric to micrometric size and tested them as positive active material in lead-acid cells. They showed that the combination of nanostructured particles and the presence of water strongly bound to the PbO_2 lattice are essential to ensure a high utilization and cycling performance of positive active material.

Recently, Yang et al. [24] combined capacity tests and XPS analysis and found a good correlation between the cycle life of positive active material and hydrated PbO_2 content.

Much speculation regarding the activity of lead dioxide exists in the literature. The majority of the authors who treated this subject concluded that chemically prepared PbO_2 is highly crystalline and less active than electrochemically prepared PbO_2 which is partially crystalline and more active. No comparative data between the two samples concerning the contribution of hydrogen in the mechanism of PbO_2 reduction are found in the literature.

In the present work and through a comparative study between two PbO_2 samples obtained by chemical and electrochemical routes, we try to understand the difference in the activity of the two samples and the contribution of hydrogen in the mechanism of PAM reduction in sulfuric acid solution. Different techniques of investigation were used.

Experimental

Preparation of samples

Chemical lead dioxide was obtained by dissolving lead tetra-acetate in distilled water. A 4.43 g of lead tetra-acetate was dissolved in 25 ml of distilled water and stirred during 30 min at room temperature.

Electrochemical lead dioxide was prepared using the conventional process. Positive paste with a density of 4.2 g cm^{-3} was prepared by mixing lead powder with water and sulfuric acid of 1.4 g cm^{-3} specific gravity (5 wt% (w/o) with respect to lead powder). This paste was applied on grids (123 × 143 × 1.6 mm) cast from Pb-Sb-Se alloy. The positive plates made from this paste were subjected to saturated steam at 65 °C and 80% of relative humidity for 1 day then air dried for another day. The plates have a porosity of 51% and the water content after "drying" is not exceeding 0.2%. Cured plates having an active mass of 106 g were first soaked for 72 h in1.40 g cm^{-3} H_2SO_4 and then formed for 20 h under a constant current of 0.5 A/plate in1.05 g cm^{-3} H_2SO_4.

The two samples of lead dioxide powders were washed in distilled water for several hours to remove the excess of electrolyte and then dried at 110 °C. They were ground in a mortar, homogenized, and set to X-ray diffraction, chemical analysis, thermal analysis, and SEM examination.

XRD characterization

The positive active materials were characterized by XRD analysis using an APD-15 Philips 2134 diffractometer with Cu $K\alpha$ radiation ($k = 1.54178$ nm). The changes in relative intensity of the X-ray characteristic diffraction lines for the different phases in PAM were adopted as a measure of the phase changes in the positive active material. It is defined as the ratio of the "I" phase characteristic reflection intensity and the sum of the intensities of the characteristic diffraction lines of all phases. Radial scans were recorded in the reflection scanning mode with 2Θ being changed from 20° to 40°.

Bragg's law, defined as $n\lambda = 2d\sin\Theta$, was used to compute the crystallographic distance (d) for the examined samples. The average crystallite size was calculated from the full width at the half maximum (FWHM) using Scherrer equation.

Thermal analysis

Thermogravimetric analysis (TGA) and differential scanning calorimetry (DSC) tests were performed using instruments supplied by Metler Toledo: TGA/SDTA 851^e and DSC 822^e, respectively. All measurements were carried out in a nitrogen atmosphere at a gas flow rate of 80 cm^3 min^{-1} for DSC and 50 cm^3 min^{-1} for TGA at a constant heating rate of 10 K min^{-1}.

Electrochemical investigations

Electrode preparation

A conductive carbon rod with a surface area of 1 cm^2 was embedded in a Teflon tube. Neat positive active material powder without additives was poured in the cavity of the electrode and hand-pressed to form a compact film of PAM around 1 mm in thickness, the film is covered with a micro-porous separator.

Electrochemical tests

All electrochemical tests were carried out in a three-electrode cell. The working electrode is at 1 cm distance from a platinum rectangular-shaped counter electrode having an apparent surface area of 5 cm^2. Hg/Hg_2SO_4/saturated K_2SO_4 is used as reference electrode. Galvanostatic discharge, cyclic voltammetry, and electrochemical impedance spectroscopy were used as techniques of investigation. All experiments were carried out at room temperature in 1.28 g cm^{-3} H_2SO_4 solution.

The electrodes were discharged at a constant cathodic current of 20 mA g^{-1}, and the potential versus capacity curves were recorded. The capacity of the PbO_2 electrode is determined.

The potential-current curves were recorded after cycling the electrodes in the potential range 1.5 to 0.5 V at a sweep rate of 50 mV s^{-1}. The capacity expressed in mAh cm^{-2} is determined by integrating the surface area of the cathodic peak corresponding to the reduction of PbO_2 to $PbSO_4$.

For each impedance measurement, a fresh PbO_2 electrode is prepared and immersed in the electrolyte. After a rest of 15 min in the solution, impedance scans were performed in the frequency range from 100 kHz to 10 mHz at a signal amplitude of 10 mV. The corresponding Nyquist plots were recorded at open-circuit potential and under cathodic polarization (900 and 800 mV, respectively).

Results and discussions

Chemical analysis

Table 1 summarizes the obtained data for the chemical composition of PbO_2 samples prepared by chemical and

Table 1 Results from chemical analysis and crystallite size calculated from FWHM method for chemical and electrochemical PbO_2

Samples	PbO_2 (%)	PbO (%)	Precipitate (%)	Crystallite size D (nm)
Chemical	79.38	–	4.58	5
Electrochemical	78.82	10.97	0.42	19

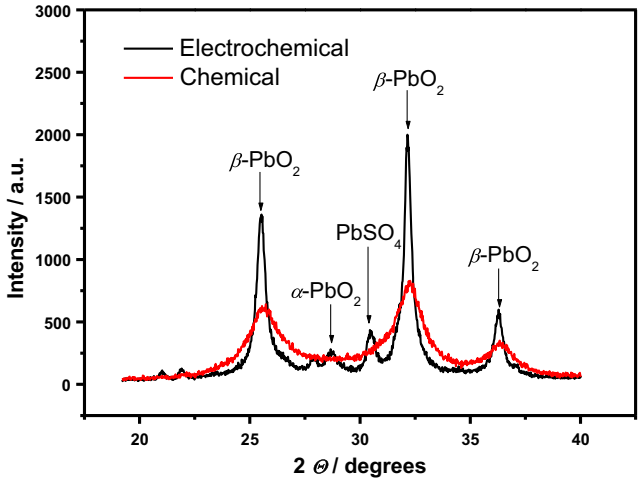

Fig. 1 XRD patterns of PbO_2 powders prepared by electrochemical and chemical routes

electrochemical routes, respectively. The data indicate that the content of PbO_2 in the two samples is the same. It represents around 80% of the total mass. The residue in the electrochemical sample is metallic lead, lead sulfate, and other additives. For the chemically prepared sample, the residue is lead oxide (not determined).

XRD analysis

As shown in Fig. 1 for both chemical and electrochemical samples, changes in peak intensity and width are observed depending on the conditions of preparation. The XRD data indicate that both samples comprise β-PbO_2 crystal phase. The XRD patterns of chemical lead dioxide powder showed that all detected peaks were identified to be β-lead dioxide. In addition of the β-phase, small amounts of α-lead dioxide (13%) and $PbSO_4$ crystals (21%) were detected in the electrochemical sample. Chemical PbO_2 yields broader peaks with low intensity, such diffractograms may be attributed to amorphous part in the phase and to H_2O incorporated in PbO_2 structure. This is also indicative of smaller crystallites. PbO_2

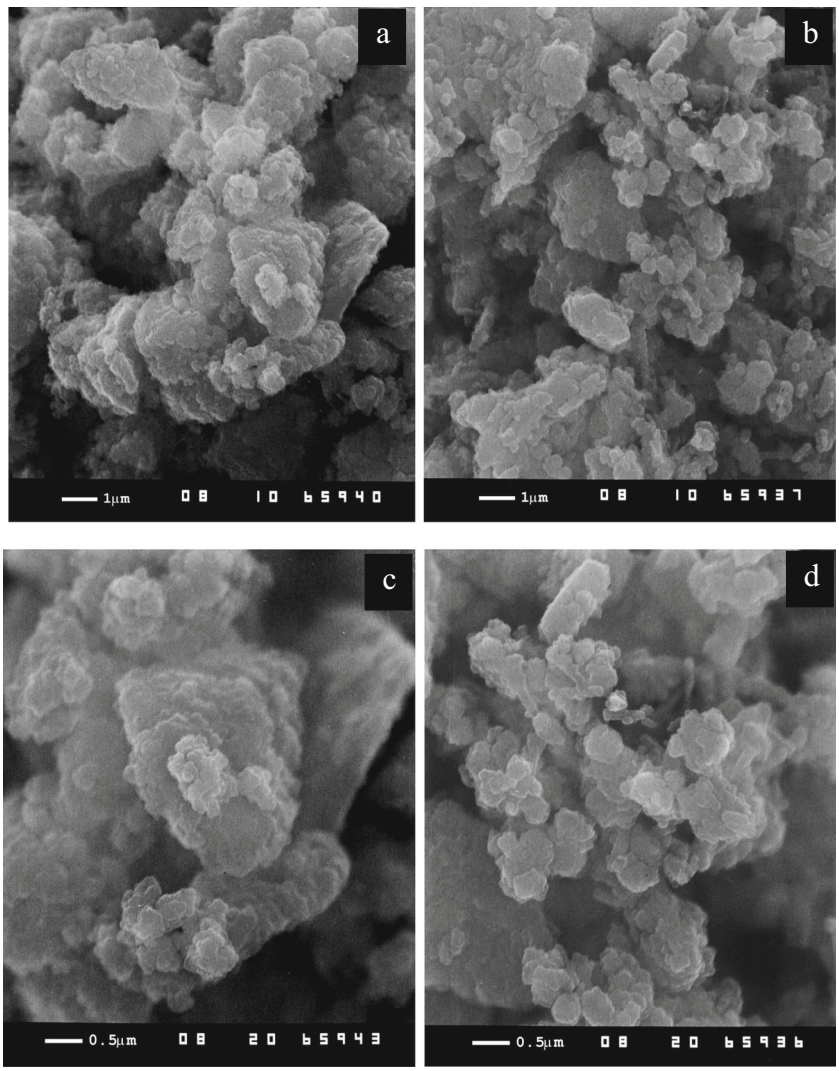

Fig. 2 Scanning electron micrographs of PbO_2 powders prepared by **a** chemical route, **b** electrochemical route, and **c**, **d** corresponding micrographs at higher magnification

prepared by the electrochemical route seems to be highly crystalline with sharp and high intensity peaks. The average crystallite size was calculated from the full width at the half maximum (FWHM) of [110] diffraction line using Scherrer equation. The difference in crystallite size value (nm) thus calculated for the different samples is reported in Table 1. The electrochemical sample yields a crystallite size (19 nm) almost four times that of the chemical PbO_2 (5 nm).

SEM examination of the microstructure of PbO_2 samples

Figure 2 presents SEM micrographs of PbO_2 particles and aggregates of PAMs prepared under different conditions. At high magnification, both chemical and electrochemical samples comprise PbO_2 particles grouped in small agglomerates, which coalesce into an aggregate. The shape and size of PbO_2 particles change from one sample to another depending on the conditions and methods of preparation. Smaller and closer interconnected PbO_2 particles in agglomerates with individual nanoparticles still distinguished are observed in the SEM examination of the chemically prepared sample (see Fig. 2c). Larger and clearly pronounced individual PbO_2 particles are obtained by the electrochemical route (see Fig. 2d).

Based on the results of SEM data, it can be generally concluded that the synthesis of lead dioxide by electrochemical or chemical methods in aqueous solution follows a precipitation-crystallization mechanism.

Thermogravimetric analysis of PbO_2 samples

The thermal analyses were performed within the temperature range from 35 to 300 °C, as the aim of these analyses was to determine the hydrated parts of the samples. Figure 3 illustrates the measured weight losses respectively for β-PbO_2 samples prepared by chemical and electrochemical routes as a function of heating temperature. Three temperature zones of weight loss, related to the dehydration of the amorphous parts of PAM, can be distinguished. A-zone: from 35 to 75 °C, in this temperature interval, the measured weight losses are due to evaporation of weakly bound (physisorbed) water. B-zone: from 75 to 150 °C, in this temperature interval, weight losses correspond to the release of H_2O from the hydrated (gel) part of PAM particles and agglomerates. C-zone: from 150 to 300 °C, weight losses at these temperatures are due to evaporation of the water that is strongly bound (chemisorbed) to the lead dioxide particles. Table 2 gives weight losses for different temperature regions and total weight loss for the investigated samples. It seems that the chemical route facilitates the hydration of the PAM and larger amounts of water are obtained for chemical β-PbO_2 compared to the electrochemical sample. For instance, the total water content in the chemically prepared sample is 5.84% and that of the sample prepared by the electrochemical route is only 2.15%.

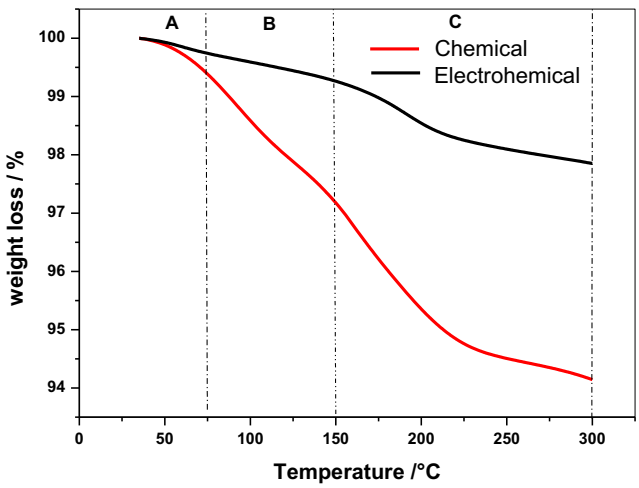

Fig. 3 Weight losses of chemical and electrochemical PbO_2

To better understand the difference in the activity between the two samples, additional data from thermal analyses were obtained. Figure 4 presents the measured heat flow as a function of the temperature for chemical and electrochemical PAM samples. For both samples, this range of temperature corresponds to the evaporation of the surface adsorbed and for strongly bounded water within the gel zones of the PAM. It is clearly seen from the thermal profiles that the endothermic and exothermic processes depend on the conditions and the method of preparation of the samples.

The endothermic peak corresponds to the departure of the water molecules adsorbed at the surface of PbO_2 particles, whereas the exothermic peak is related to the dehydration of the amorphous parts of PbO_2. When heated, amorphous lead dioxide lattice is reordered under oxygen evolution and combined water. This exothermic reaction is associated with a reduction of Pb^{4+} to Pb^{2+} according to Eqs. (5) and (6), respectively:

$$OH^- + OH^- \rightarrow {}^1/_2\, O_2 + H_2O + 2e^- \quad (5)$$

$$Pb^{4+} + 2e^- \rightarrow Pb^{2+} \quad (6)$$

The thermal profile for chemical PbO_2 is characterized with broad peaks corresponding with its high amorphous microstructure and larger content of water in the sample. For electrochemical PbO_2, representative thermal profile is characterized with sharp peaks with low intensity related to its low amorphous structure and lower content of water.

Table 2 Weight losses of PAM prepared by chemical and electrochemical routes

Weight loss (%)	A-zone	B-zone	C-zone	Total
Chemical	0.61	2.20	3.03	5.84
Electrochemical	0.26	0.48	1.41	2.15

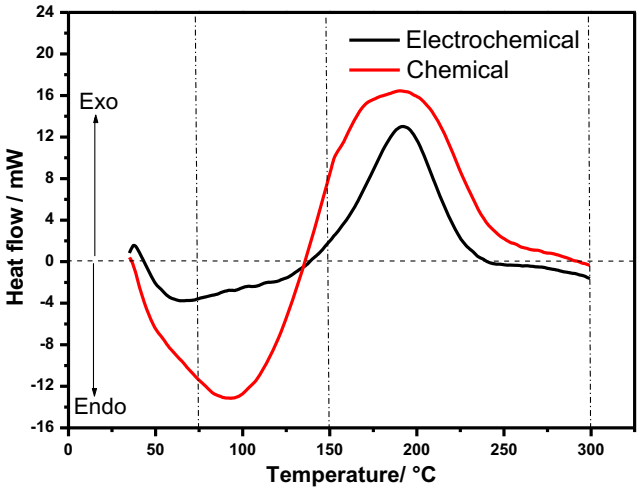

Fig. 4 DSC curves of chemical and electrochemical PbO_2

Electrochemical investigations

Galvanostatic discharge

The discharge curves of chemical and electrochemical PbO_2 are presented in Fig. 5. We report the change in potential versus the capacity of the electrode expressed in mAh g^{-1}. From the zoom insert in Fig. 5, we can see that chemical PbO_2 presents an open-circuit potential slightly higher ($E_{i=0}$ = 1025 mV) than that of PbO_2 prepared by electrochemical route ($E_{i=0}$ = 993 mV). Consequently, this yields to a potential plateau that corresponds to the reduction of PbO_2 to $PbSO_4$ slightly higher. This is due to the difference in the micromorphology and crystallite size of PbO_2 particles. It is commonly known that the capacity of lead dioxide depends on the water content, but although the chemical sample exhibits small crystallite size and amorphous character, we notice that the capacity of the electrochemical sample is much higher (70 mAh g^{-1}) than that of the chemical sample (50 mAh g^{-1}).

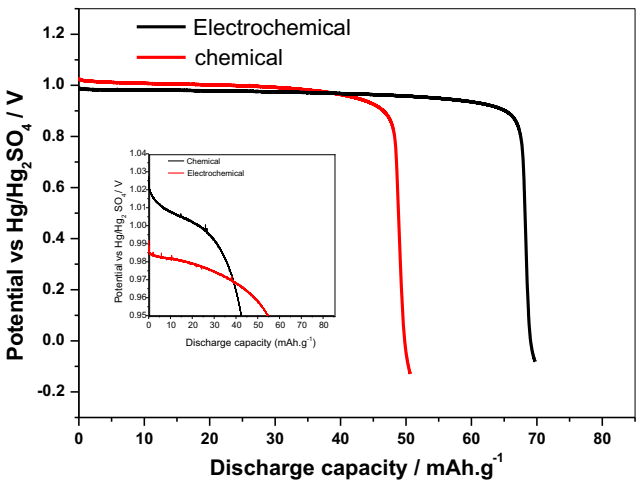

Fig. 5 Discharge capacity of chemical and electrochemical PbO_2 samples

Cyclic voltammetry

In Fig. 6, we report the evolution in current density versus the electrode potential after 100 cycles at a sweep rate of 50 mV s^{-1}. From these voltammograms, it is clearly deduced that PbO_2 prepared by the electrochemical method presents higher cathodic and anodic current densities that correspond respectively to the reduction of PbO_2 to $PbSO_4$ during discharge and to the oxidation of $PbSO_4$ to PbO_2 during charge. The capacity versus the number of cycles for both samples is illustrated in Fig. 7. We can see that the increase in capacity for PbO_2 prepared by the electrochemical process is more important compared to that of the sample chemically produced. The capacity values of the two samples determined for the 100th cycle are equal to 15.1 and 22.2 mAh g^{-1}, respectively, for chemically prepared and electrochemically prepared PbO_2.

Consequently, the electrochemical route seems to facilitate the production of positive active material with higher performance cycling. In contrast, the chemical method exhibits lower PAM cycling.

Electrochemical impedance spectroscopy

Typical Nyquist diagrams were obtained at open-circuit potential (OCP) and under cathodic polarization for both samples prepared by chemical and electrochemical routes. The experimental plots and their corresponding equivalent electrical circuits are represented in Fig. 8.

At open-circuit potential, one semicircle is observed at high frequency corresponding to charge transfer resistance and double-layer capacitance formation. Under cathodic polarization, it can be observed that chemical PbO_2 electrode shows an important increase in the diameter of the semicircle and capacitance value as compared to electrochemical PbO_2 electrode (see Fig. 8a, b).

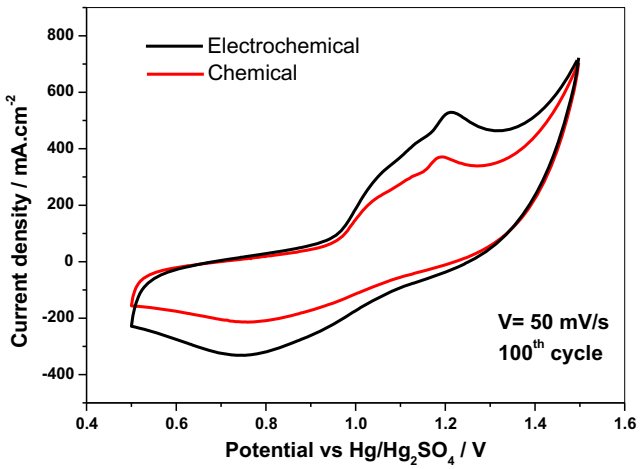

Fig. 6 Cyclic voltammetry curves for the 100th cycle of chemical and electrochemical PbO_2

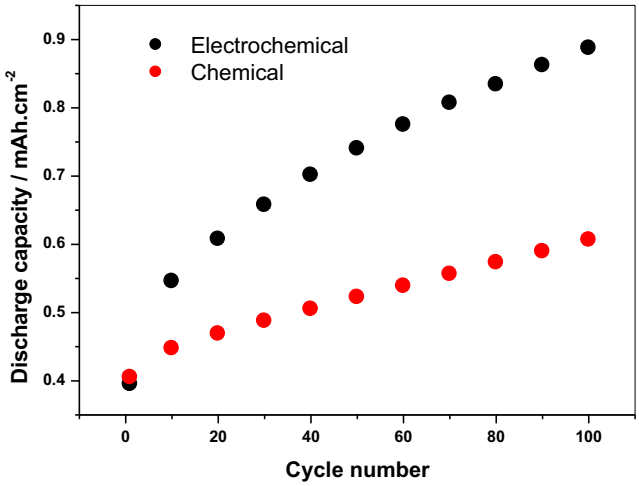

Fig. 7 Cycling performance of investigated β-PbO_2 samples versus cycle number

The EIS data of the electrodes tested at different potentials fit the circuit equivalent R_s (R_{ct}, Q), where R_s is the solution resistance, R_{ct} is the charge transfer resistance of the PbO_2 electrode, and Q is the constant phase element (*CPE*). The corresponding simulated data are summarized in Table 3.

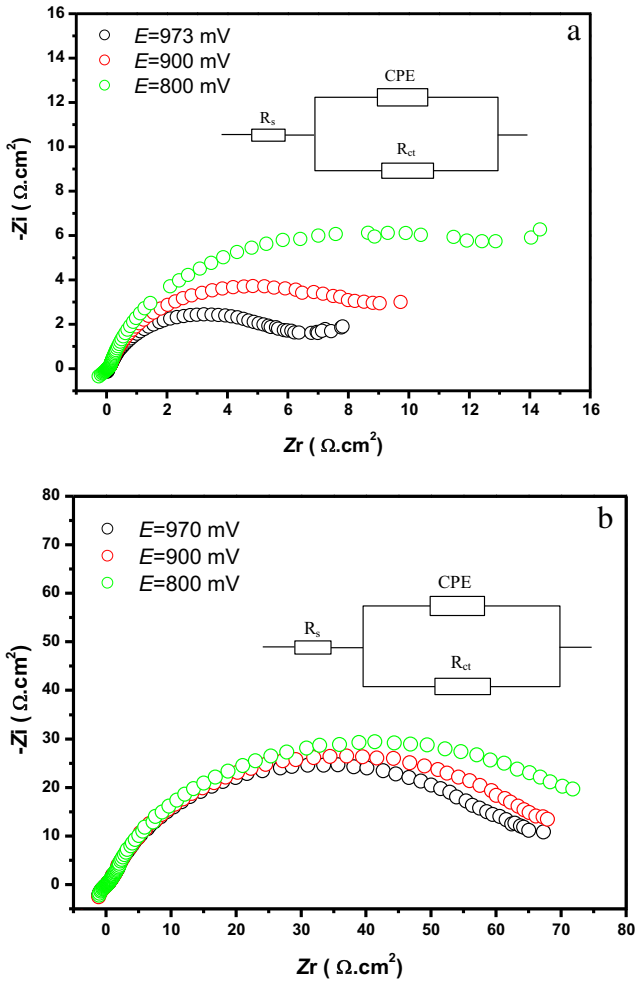

Fig. 8 Nyquist diagrams at open-circuit potential (OCP) and under cathodic polarization for PbO_2 samples: **a** chemical and **b** electrochemical. Inset equivalent electrical circuit

The data present the variation of the charge transfer resistance with the cathodic polarization applied to both PAMs. It is clearly seen that chemical PbO_2 with small crystallite size and high water content presents small values of charge transfer resistance. Both samples show an increase of the charge transfer resistance with the increase of the value of the potential of polarization. This could be explained by the fact that under polarization amorphous particles, surfaces are partially converted to $PbSO_4$ leading to higher resistance.

The data of the increase of the charge transfer resistance (expressed in percentage (%) with respect to the initial value of the resistance measured at OCP) with the potential of polarization are reported in Table 4. The data show clearly the remarkable effect of cathodic polarization on the activity and electrical properties of the two samples. In fact and although chemical PbO_2 particles are smaller and exhibit more amorphous character, i.e., high structural water content, as compared to electrochemical PbO_2 ones but during discharge, they yield low electrical conductivity and smaller value of capacity. This is in disagreement with the data published in our previous work [22]. In this paper, we showed that the mechanism of PbO_2 reduction could be expressed as a double-injection process of electron and proton according to the following equation:

$$<> + H^+ + e^- \rightarrow < H > \quad (7)$$

where <> and <H> denote the free and hydrogen occupied sites, respectively.

We demonstrated also a good correlation between the capacity of PAM and the content of structural water. When heating lead dioxide, the departure of water affects not only the capacity of PAM but also its electrical properties. This leads to a capacity loss and a decrease in the values of D_{H^+} (proton diffusion coefficient).

Table 3 Simulated data of the EIS parameters for chemical and electrochemical PbO_2 electrodes

	R_s (Ω cm^2)	R_{ct} (Ω cm^2)	Q (Ω^{-1} cm^2 s^n)	n
Chemical PbO_2				
E = 973 mV	0.10	06.48	0.083063	0.82
E = 900 mV	0.13	09.15	0.084747	0.86
E = 800 mV	0.12	15.27	0.081832	0.85
Electrochemical PbO_2				
E = 970 mV	0.71	65.93	0.0054814	0.81
E = 900 mV	0.44	72.03	0.0054519	0.80
E = 800 mV	0.64	79.45	0.0084016	0.81

Table 4 Variation of the increase in charge transfer resistance (%) with the change of the potential of polarization calculated from impedance values of PAM prepared by chemical and electrochemical routes

Potential of polarization (mV)	Increase in charge transfer resistance (%) chemical PbO_2	Increase in charge transfer resistance (%) electrochemical PbO_2
900	41.2	9.25
800	135.6	20.5

From these findings, one can suggest that the electrochemical route based on a longtime process yields a PAM with a gel-crystal microstructure and a homogeneous and ordered repartition of the hydroxyl groups and/or water molecules. These facilitate the diffusion of the protons during discharge and charge of PAM and favorite the increase of the capacity of PbO_2 during cycling. In the contrary, the chemical method based on a short-time process leads to a PAM with an amorphous part in the crystal microstructure and a heterogeneous and disordered distribution of the hydroxyl groups and/or water molecules. Obviously, chemical PbO_2 is less active than the electrochemical sample. To our knowledge, this is the key point that could explain the difference in electrochemical activity between β-PbO_2 prepared by chemical and electrochemical route.

Conclusion

The experimental basis gained from this manuscript is the combining of thermal analysis with the different electrochemical techniques to try to explain the difference in electrical performance for the two samples. The activity of lead dioxide in sulfuric acid depends not only on the quantity of structural water but also on the way these hydrogen species are arranged in the amorphous part of PbO_2.

Electrochemical lead dioxide is more active in sulfuric acid than that prepared by chemical route. Thermal analysis and electrochemical impedance spectroscopy are the key techniques investigated in this work to better understand this difference in activity between the two samples. More precisely, this activity may be probably due to the well and homogeneous repartition of the free hydrogen sites within the structure of electrochemical PbO_2. These free hydrogen sites facilitate the diffusion of the proton and lead to PbO_2 with high capacity.

In contrast, the heterogeneous and randomly repartition of the free hydrogen sites within the structure of chemical PbO_2 limits the diffusion of the proton and consequently gives a PAM with low capacity.

These findings explain why the chemical phase is less active and yields small capacity with cycling compared to PAM prepared by the conventional process.

References

1. Rüetschi P, Cahan BD (1957) Anodic corrosion and hydrogen and oxygen overvoltage on lead and lead antimony alloys. J Electrochem Soc 104(7):406–413. https://doi.org/10.1149/1.2428614
2. Burbank J (1957) Anodization of lead and lead alloys in sulfuric acid. J Electrochem Soc 104(12):693–701. https://doi.org/10.1149/1.2428455
3. Rüetschi P (1963) Stability and reactivity of lead oxides. Electrochim Acta 8(5):333–342. https://doi.org/10.1016/0013-4686(63)80063-8
4. Bagshaw NE, Clarke RL, Halliwell B (1966) The preparation of lead dioxide for X-ray diffraction studies. J Appl Chem 16:180–184
5. Duisman JA, Giaugue WF (1968) Thermodynamics of the lead storage cell. The heat capacity and entropy of lead dioxide from 15 to 318.degree K. J Phys Chem 72(2):562–573. https://doi.org/10.1021/j100848a030
6. Caulder SM, Simon AC (1974) Thermal decomposition mechanism of formed and cycled lead dioxide electrodes and its relationship to capacity loss and battery failure. J Electrochem Soc 121:1546–1551
7. Turner AD, Moseley PT, Hutchison JL (1984) Utilization of active material in PbO_2 electrodes. Proc Electrochem Soc 84-14:267–276
8. Taylor EJ, Shia GA, Peters DT (1984) A precharged positive plate for lead-acid automotive battery: I. Positive plate allowing direct incorporation of PbO_2. J Electrochem Soc 131(3):483–487. https://doi.org/10.1149/1.2115613
9. Taylor EJ, Shia GA, Peters DT (1984) A precharged positive plate for lead-acid automotive battery: II. Effects of various PbO_2 types and paste formulations on precharged positive plate performance. J Electrochem Soc 131(3):487–491. https://doi.org/10.1149/1.2115614
10. Moseley PT, Bridger NJ (1984) Lead-acid battery cathodes incorporating chemically prepared PbO_2. J Electrochem Soc 131(3):608–610. https://doi.org/10.1149/1.2115634
11. Hill RJ, Jessel AM (1987) The electrochemical activity of PbO_2. A nuclear magnetic resonance study of hydrogen in battery and chemically prepared material. J Electrochem Soc 134(6):1326–1330. https://doi.org/10.1149/1.2100667
12. Tokunaga A, Tsubota M, Yonezu K, Ando K (1987) Effect of anisotropic graphite on discharge performance of positive plates in pasted-type lead-acid batteries. J Electrochem Soc 134(3):525–529. https://doi.org/10.1149/1.2100503
13. Rüetschi P (1992) Influence of crystal structure and interparticle contact on the capacity of PbO_2 electrodes. J Electrochem Soc 139(5):1347–1351. https://doi.org/10.1149/1.2069410
14. Pavlov D (1992) The lead-acid battery lead dioxide active mass: a gel-crystal system with proton and electron conductivity. J Electrochem Soc 139(11):3075–3080. https://doi.org/10.1149/1.2069034
15. Pavlov D, Balkanov I, Halachev T, Rachev P (1989) Hydration and amorphization of active mass PbO_2 particles and their influence on the electrical properties of the lead-acid battery positive plate. J Electrochem Soc 136(11):3189–3197. https://doi.org/10.1149/1.2096424
16. Monahov B, Pavlov D (1993) Hydrated structures in the anodic layer formed on lead electrodes in H_2SO_4 solution. J Appl Electrochem 23:1244–1250
17. Fitas R, Chelali N, Zerroual L, Djellouli B (2000) Mechanism of the reduction of α- and β-PbO_2 electrodes using an all-solid-state system. Solid State Ionics 127(1–2):49–54. https://doi.org/10.1016/S0167-2738(99)00266-0
18. Hill RJ, Houchin MR (1985) Incorporation of hydrogen in lead dioxide by a surface hydrolysis mechanism. Electrochim Acta 30(4):559–561. https://doi.org/10.1016/0013-4686(85)80047-5

19. Fitas R, Zerroual L, Chelali N, Djellouli B (1996) Heat treatment of α- and β-battery lead dioxide and its relationship to capacity loss. J Power Sources 58(2):225–229. https://doi.org/10.1016/S0378-7753(96)02372-5
20. Fitas R, Zerroual L, Chelali N, Djellouli B (1997) Role of hydration water in the reduction process of PbO_2 in lead/acid cells. J Power Sources 64(1-2):57–60. https://doi.org/10.1016/S0378-7753(96)02502-5
21. Fitas R, Zerroual L, Chelali N, Djellouli B (2000) Thermal degradation of α- and β-PbO_2 and its relationship to capacity loss. J Power Sources 85(1):56–58. https://doi.org/10.1016/S0378-7753(99)00382-1
22. Zerroual L, Fitas R, Djellouli B, Chelali N (2006) Relationship between water departure and capacity loss of α and β-PbO_2 using an all solid-state system: estimation of proton diffusion coefficient. J Power Sources 158(2):837–840. https://doi.org/10.1016/j.jpowsour.2005.11.011
23. Morales J, Petkova G, Cruz M, Caballero A (2006) Synthesis and characterization of lead dioxide active material for lead-acid batteries. J Power Sources 158:831–836
24. Yang S, Li R, Cai X, Xue K, Yang B, Hu X, Dai C (2017) Influence of hydrated PbO_2 content on the cycling performance of lead-acid batteries. J Electrochem Soc 164(9):A2007–A2011. https://doi.org/10.1149/2.1261709jes